Nonuniform Contribution of Internal Variability to Recent Arctic Sea Ice Loss

MARK ENGLAND

Applied Physics and Applied Mathematics Department, Columbia University, New York, New York

ALEXANDRA JAHN

Department of Atmospheric and Oceanic Sciences, and Institute of Arctic and Alpine Research, University of Colorado Boulder, Boulder, Colorado

LORENZO POLVANI

Applied Physics and Applied Mathematics Department, and Department of Earth and Environmental Science, Lamont Doherty Earth Observatory, Columbia University, New York, New York

ABSTRACT

Over the last half century, the Arctic sea ice cover has declined dramatically. Current estimates suggest that, for the Arctic as a whole, nearly one-half of the observed loss of summer sea ice cover is not due to anthropogenic forcing but rather is due to internal variability. Using the 40 members of the Community Earth System Model Large Ensemble (CESM-LE), our analysis provides the first regional assessment of the role of internal variability on the observed sea ice loss. The CESM-LE is one of the best available models for such an analysis, because it performs better than other CMIP5 models for many metrics of importance. Our study reveals that the local contribution of internal variability has a large range and strongly depends on the month and region in question. We find that the pattern of internal variability is highly nonuniform over the Arctic, with internal variability accounting for less than 10% of late summer (August–September) East Siberian Sea sea ice loss but more than 60% of the Kara Sea sea ice loss. In contrast, spring (April–May) sea ice loss, notably in the Barents Sea, has so far been dominated by internal variability.

1. Introduction

The rapid loss of Arctic sea ice over the last 50 years has been one of the most alarming signals of a changing climate. September sea ice extent has decreased by roughly 50% since 1979 (Comiso et al. 2017; Stroeve and Notz 2018). Current model projections show that a summer ice-free Arctic before 2100 is very likely unless future warming is limited to 1.5°C or less (Jahn 2018; Niederdrenk and Notz 2018; Sigmond et al. 2018) and is likely to occur by the middle of this century if anthropogenic emissions continue on the current trajectory (Overland and Wang 2013; Liu et al. 2013; Jahn et al. 2016; Jahn 2018; Sigmond et al. 2018). Furthermore,

over recent decades the Arctic melt season has lengthened (Stroeve et al. 2014a) and sea ice cover has undergone considerable thinning (Kwok and Rothrock 2009; Stroeve et al. 2014b; Lindsay and Schweiger 2015; Kwok 2018).

These changes in sea ice are both strongly regionally and seasonally dependent. For example, sea ice loss in the Beaufort, Chutchi, Laptev, and East Siberian Seas has been concentrated in the late summer, whereas sea ice loss in the Barents, Okhotsk, and Baffin Seas has primarily occurred in the winter and springtime (Onarheim et al. 2018). Sea ice concentration changes have been occurring primarily at the ice margins where ice is thinner. Understanding the changes of Arctic sea ice, especially on a regional scale, is becoming increasingly critical for many sectors of business and society (Lahn and Emmerson 2012; Barnhart et al. 2016). To improve our ability to anticipate future Arctic sea ice change, it is important to estimate how much of the observed change in sea ice in different Arctic basins is attributable to

increased anthropogenic emissions, and how much is due to internal variability of the climate system.

Internal variability represents the random fluctuations inherent in the climate system, related to naturally occurring changes in the large-scale atmospheric and ocean circulation, which can strengthen or mitigate the trends associated with human induced climate change over time scales from years to several decades. Recent estimates suggest that internal variability has contributed up to 50% of the observed trend in September pan-Arctic sea ice extent decline in recent decades [44% (Kay et al. 2011), 43%–53% (Stroeve et al. 2007), 33%–48% (Stroeve et al. 2012), 49% (Zhang 2015), 30%–50% (Ding et al. 2017), 33% (Ding et al. 2019)]. Furthermore, internal variability has been used to project a slowdown in Atlantic Ocean sea ice loss in the coming decade (Yeager et al. 2015). Although there is broad agreement on the importance of internal variability for recent Arctic-wide aggregate sea ice changes, much less is known about its role in different Arctic basins and at different times of the year. Hence the key question we address here: Is the contribution of internal variability to the observed sea ice loss uniform in time and space across the Arctic, or is it confined to specific regions or specific times of the year?

In this paper we answer this question using the 40 members of the Community Earth Systems Model Large Ensemble (CESM-LE) (Kay et al. 2015), complemented by model results from phase 5 of the Coupled Model Intercomparison Project (CMIP5) archive. Several studies have used the CESM-LE to investigate the effect of internal variability on pan-Arctic sea ice extent (Swart et al. 2015; Jahn et al. 2016; Jahn 2018) but ours is the first attempt to examine the regional and temporal features of internal variability for sea ice concentration. We first show that the CESM-LE is able to faithfully capture the regional structure of year-to-year sea ice concentration variability (section 2d), especially when compared with ensembles of other CMIP5 models that exhibit large biases. We then assess the contribution of internal variability to observed trends in two seasons; the spring and summer (section 3). We will show that, in summer, the role of internal variability is nonuniform; internal variability accounts for a quarter to a half of the sea ice loss in most regions, but in some specific hotspots internal variability is the dominant factor. In spring, our results show that internal variability accounts for the vast majority of observed sea ice loss to date.

2. Data and methods

a. Observational data

The observational dataset used for Arctic sea ice concentrations in this study is the Met Office Hadley Centre Sea Ice and Sea Surface Temperature dataset, version 2.1 (HadISST2.1.0.0) (Titchner and Rayner 2014). Passive microwave data from satellites are combined with historical sources such as sea ice charts to estimate Arctic sea ice concentrations back to 1850 on a regular 1° by 1° grid. The period of interest for this study starts at 1958 so as to cover a 50-yr range with decadal averages. There is a higher degree of confidence in the variability of Arctic sea ice after 1953; prior to this, mostly climatological values are used (Titchner and Rayner 2014).

b. Model simulations

The 40 members of the CESM-LE (Kay et al. 2015) are ideally suited to answer questions regarding the role of internal variability. All the members of this ensemble are forced with identical historical forcing for 1920–2005 (Lamarque et al. 2010) and future emissions under the RCP8.5 scenario for the years 2006–2100 (Meinshausen et al. 2011). The difference between the 40 members solely arise from random fluctuations generated by roundoff-level perturbations in the initial conditions of the air temperature field. As such, each member represents an independent realization of the climate system, and the spread represents uncertainty arising from internal variability alone. We also utilize the 1800 years of the preindustrial 1850 control run (Kay et al. 2015) with the same version of CESM1-CAM5 (Hurrell et al. 2013) to estimate the magnitude of internal variability without the presence of anthropogenic emissions.

We compare results from the CESM-LE with simulations from CMIP5 (Taylor et al. 2012) in section 2d. To assess the interannual variability of sea ice concentration we select the seven models that have at least four members (viz., CCSM4, CNRM-CM5, CSIRO Mk3.6.0, EC-EARTH, HadGEM2-ES, IPSL-CM5A-LR, and MIROC5; expansions of model names and institutions can be found at https://www.ametsoc.org/PubsAcronymList). To sample as much of the internal variability as possible, we also utilize the 50 members of the CanESM2 large ensemble instead of the 5 members of CanESM2 from the CMIP5 ensemble. To investigate sea ice extent trends and changes in the multimodel mean (section 3a), we use the first member from each of the 32 CMIP5 models for which we had access to the necessary data. We only use one ensemble member to avoid biasing the multimodel mean toward any one model. We note that averaging across CMIP5 models conflates internal variability with structural uncertainty so caution should be used when directly comparing the CMIP5 multimodel mean with the mean of a single model large ensemble.

c. Change in decadal averages

In this study we will focus on 50-yr differences in decadally averaged Arctic sea ice concentration in order

to examine the contribution of internal variability to long-term, multidecadal changes in Arctic sea ice. In particular, we are interested in the decade 1958–67, which occurs before significant amounts of Arctic sea ice loss, and the most recent decade 2008–17, which has seen large amounts of sea ice loss. These two decades are one-half of a century apart. Using linear regression, as done by most previous studies (e.g., Kay et al. 2011; Stroeve et al. 2012), is usually a more powerful approach (Barnes and Barnes 2015). However, we here examine epoch differences so as not to assume that changes have been linear in time. In fact, as will be shown below, the rate of sea ice loss has accelerated since 1990. Hence, the assumption of linearity since the middle of the twentieth century may not be valid.

d. Evaluation of internal variability

To study the contribution of internal variability to recent changes in Arctic sea ice, we need a model that realistically simulates both the present Arctic sea ice conditions and its internal variability. The CESM-LE has been shown to realistically simulate present-day Arctic sea ice thicknesses and matches the observed seasonal cycle of Arctic sea ice extent very well [see Figs. S1 and S2 of Jahn et al. (2016) as well as Labe et al. (2018)]. As the observations are only one realization, it is not possible to assess the realism of the simulated multidecadal internal variability from the observational record. However, previous studies have shown that interannual variability is a suitable proxy for investigating internal variability on longer time scales (Thompson et al. 2015). This technique is only suitable if the variability is stationary in time. We caution against using this technique for studying future sea ice loss because the variability is projected to substantially change [see Fig. S5 of Jahn (2018)]. Here, under the assumption of stationarity, we assess interannual variability in the CESM-LE to assess the accuracy of the simulated internal variability.

The interannual variability is here calculated as the standard deviation σ of the linearly detrended sea ice concentration time series, covering the 60 years from 1958 to 2017, which we shall hereinafter refer to as the "historical period," in each grid box. When more than one realization exists (i.e., when not analyzing the observational record), we linearly detrend each member, take the standard deviation of the time series, and then average across the ensemble members. To mitigate issues associated with comparing one time series and the average of an ensemble of time series, we utilize the approach of McKinnon et al. (2017) and McKinnon and Deser (2018) and use a false discovery rate of 10% with a two-tailed Student's t distribution.

The overall spatial structure of the interannual variability of the CESM-LE over the historical period is very similar to the observations (cf. top and middle row of Fig. 1), but the magnitude of the variability is underestimated by the model, in particular in the northernmost regions where the model variability is nearly one-half of that observed in August–September (Fig. 1f). However, when compared with all other CMIP5 model, which have at least four ensemble members (Fig. 2), the CESM-LE produces the most realistic spatial structure and magnitude of interannual sea ice variability. In particular, in August–September most other models either simulate too much variability over the Arctic Ocean, or cannot capture the correct magnitude of variability near to the coastline. The pattern correlation coefficients with the observations are shown in red, with the CESM-LE being the most similar (0.94). We note that, however, pattern correlation is not a perfect metric because it only takes into account the spatial pattern and not the magnitude. Therefore CCSM4 and EC-EARTH have high correlation coeffcients even if the magnitude of sea ice variability is too high. In April–May, the CMIP5 models are able to better capture the observed structure of internal variability than in August–September, but even for April–May the CESM-LE still performs well relative to the other models (Fig. 3). The CESM-LE has the joint highest pattern correlation score with the observations (0.8), along with EC-EARTH, which has too much variability in the Barents Sea. From this analysis we conclude that, although it is only one model, the CESM-LE is one of the best available models with enough ensemble members to study the contribution of internal variability to recent changes in sea ice on a regional scale.

e. Separating forced versus internal variability

To quantify the contribution of internal variability to recent Arctic sea ice changes on a regional scale, we separately calculate the forced contribution Δ_{forced} and the contribution of internal variability Δ_{iv} to the sea ice loss, for each grid box in the CESM-LE. The histograms in Fig. 4 illustrate this calculation for one grid box in the East Siberian Sea. The forced contribution, Δ_{forced}, is defined as the ensemble mean change (either from the 40 members of the CESM-LE or the CMIP5 multimodel ensemble). The ensemble mean change from a single model is shown to be a good estimate of the forced signal (Frankcombe et al. 2018). We have checked that the ensemble of a bootstrapped distribution of 50-yr changes from the 1800-yr-long preindustrial control run is centered on zero to ensure that there is no model drift. The contribution of internal variability, Δ_{iv}, is the remainder of the observed change after Δ_{forced} is
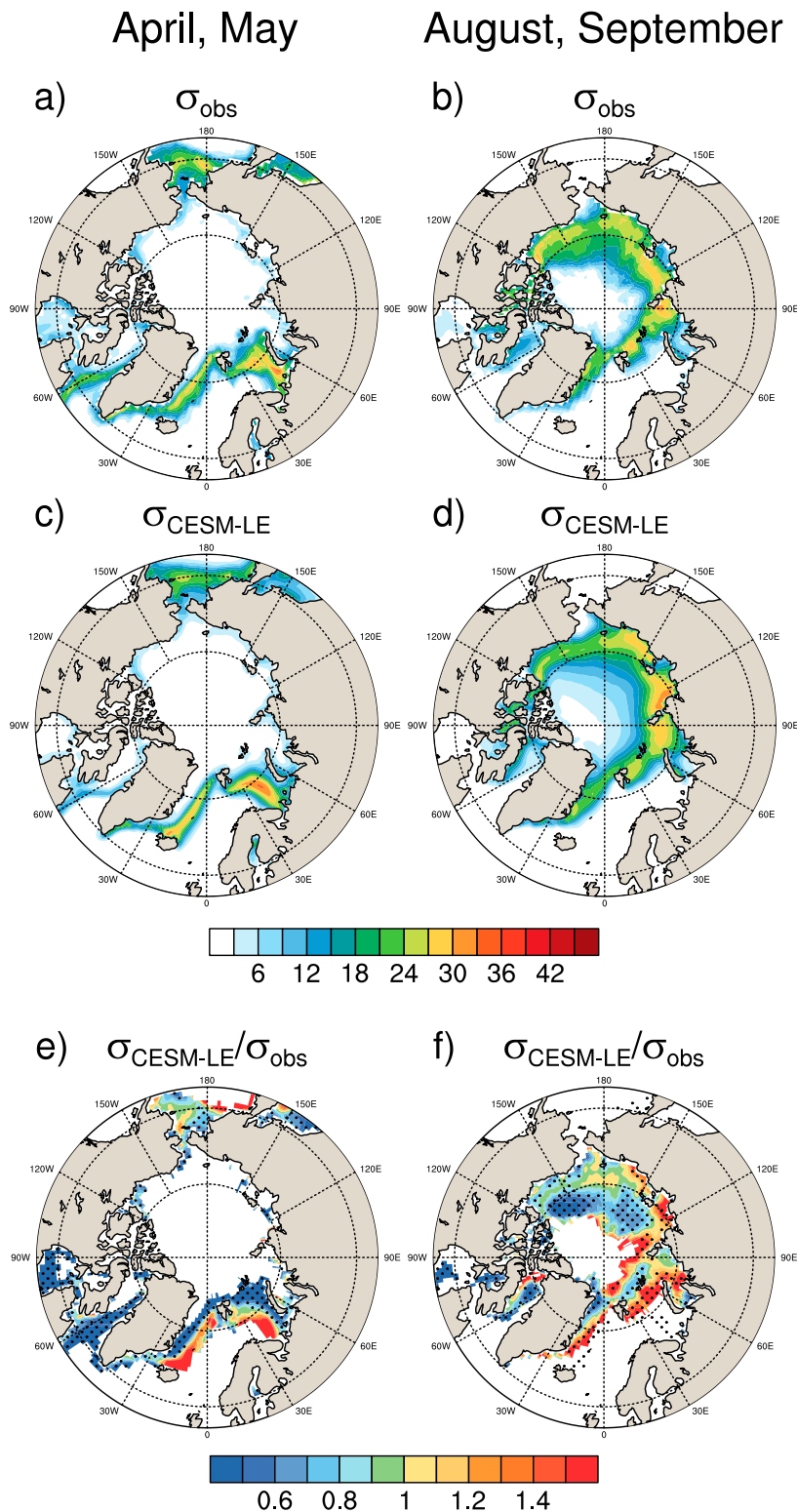
FIG. 1. Standard deviation of linearly detrended (left) April–May and (right) August–September sea ice fraction values over 1958–2017 from (a),(b) the HadISST observational dataset and (c),(d) the 40 members of the CESM-LE. (e),(f) The ratio of the two is shown for regions, and the stippling indicates differences that are significant using a false detection rate of 10%. Blue and red indicate that the CESM-LE under- and overestimates, respectively, the observed standard deviation.
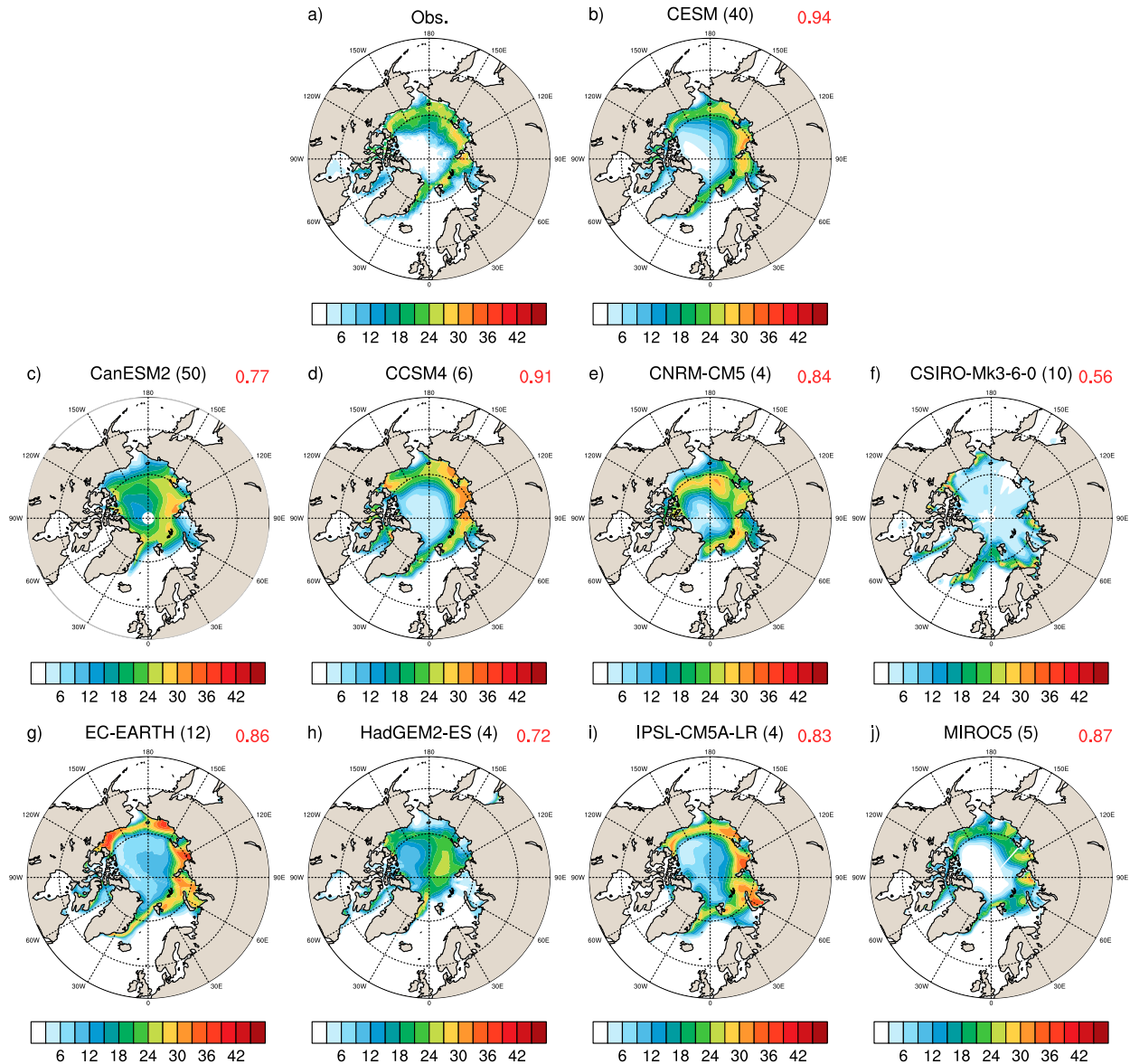
FIG. 2. Standard deviation of linearly detrended August–September sea ice concentration values 1958–2017 from (a) the HadISST observational dataset, (b) the 40 members of the CESM-LE, and (c)–(j) 8 CMIP5 models (CanESM2, CCSM4, CNRM-CM5, CSIRO Mk3.6.0, EC-EARTH, HadGEM2-ES, IPSL-CM5A-LR, and MIROC5). These are the CMIP5 models that have four or more ensemble members for the historical period, with the number of members displayed in parentheses after the model name. The pattern correlation score with observations is shown in red for each model.

subtracted out. Internal variability can also be expressed as a percentage contribution of the observed sea ice loss: $100 \times [|\Delta_{iv}|/(\Delta_{iv} + \Delta_{forced})]$.

3. Results

a. Pan-Arctic sea ice trends and internal variability

We first examine the aggregate Arctic-wide changes in the CESM-LE to allow for comparison with previous studies. In this study we focus our analysis on two 2-month periods: April–May and August–September. We select these months to highlight the contrasting role of internal variability in different seasons, and the late summer is of particular interest because that is the season of the most rapid sea ice loss. The months were paired into two-month groupings because results from the individual months were qualitatively similar.

In April–May, the observed long-term trend (>30 yr) in sea ice extent from 1958 lies outside the trends
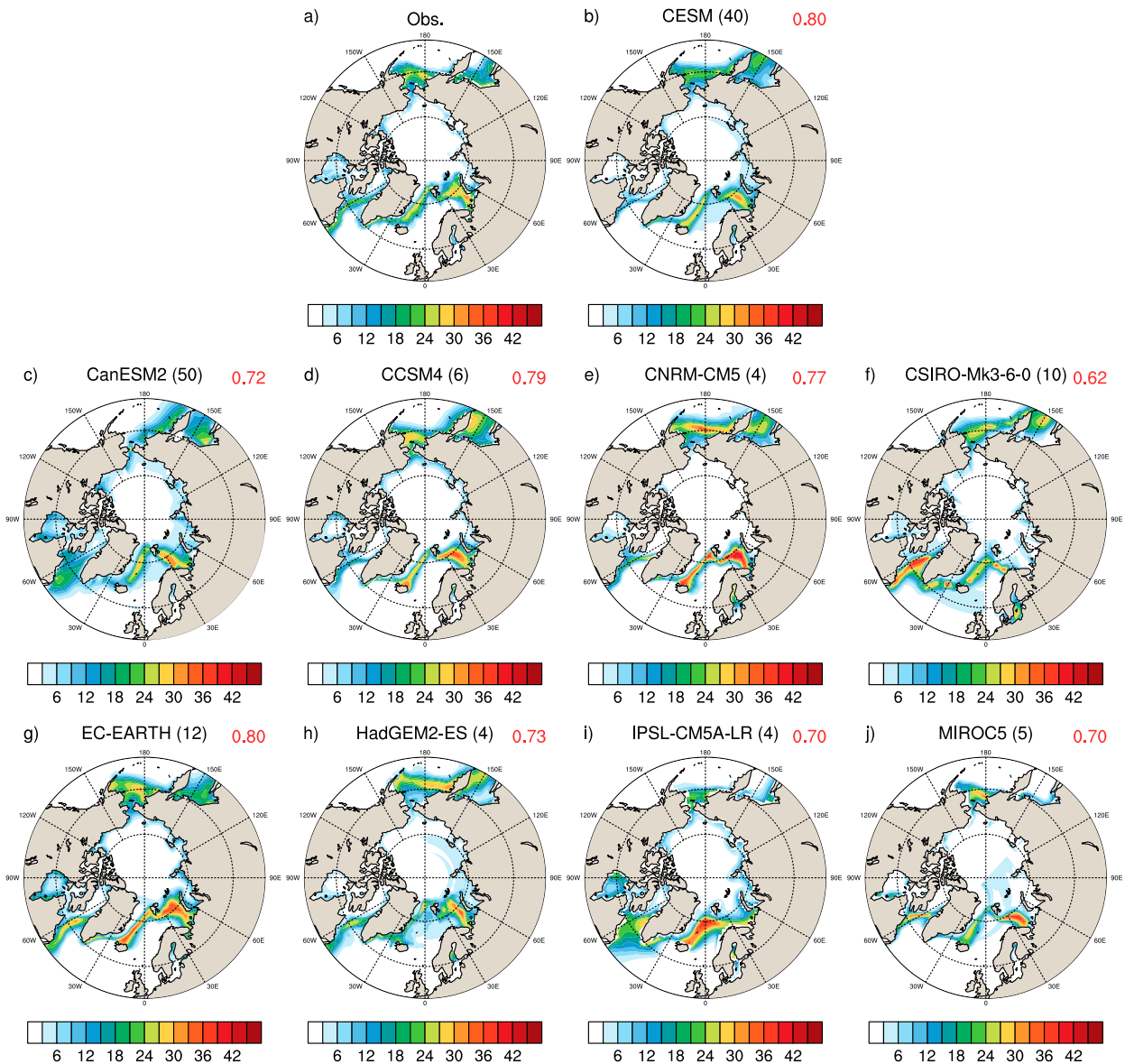
FIG. 3. As in Fig. 2, but for April–May.

simulated by the CESM-LE (Fig. 5) but the shorter 20-yr trends compare well with observations (Fig. 6). In August–September, the observed long-term trend in sea ice extent is within the range of trends simulated by the CESM-LE (Fig. 5) and the shorter 20-yr trends are also within the spread, except for the trends ending after 2010 (Fig. 6). (Results for each pair of months for the whole year are shown in Figs. S2 and S3 in the online supplemental material.) We note that June and July are the months where the CESM-LE is not able to capture the shorter or longer term trends in observed sea ice extent when the sea ice loss over the last decade is included (Figs. S2 and S3). These results demonstrate that

whether the observed trend is found to lie within the CESM-LE or CMIP5 ensemble spread is dependent on the season, trend length, and chosen end year.

For the pan-Arctic sea ice loss since 1979 in September, the CESM-LE shows a contribution from internal variability to the observed trend of 33% (Ding et al. 2019) [the ensemble mean trend is $-0.60 \times 10^6 \, \text{km}^2$ $(10\,\text{yr})^{-1}$ as compared with the observed trend of $-0.91 \times 10^6 \, \text{km}^2 \, (10\,\text{yr})^{-1}$]. To account for atmospheric conditions that are found to precede September sea ice loss, Ding et al. (2019) use a pattern scaling technique with the CESM-LE to suggest that internal variability is in fact responsible for 47%–57% of the observed
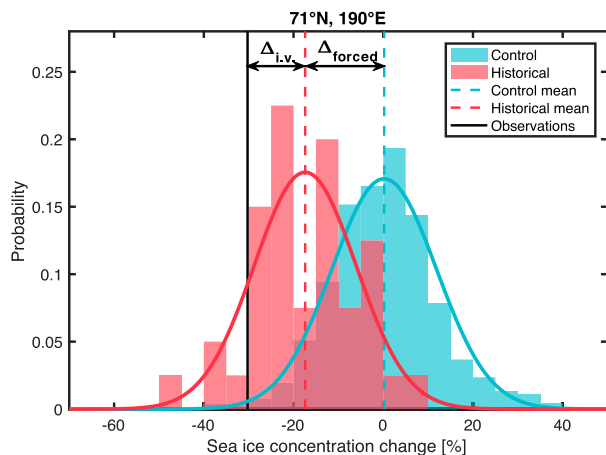
FIG. 4. The histograms are the distributions of 50-yr changes in decadal means from the 1800-yr CESM control run and the 40 members of the CESM-LE historical simulations for one gridbox (71°N, 190°E). The contribution of internal variability in each grid box is calculated as $100 \times [|\Delta_{iv}|/(\Delta_{iv} + \Delta_{forced})]$.

sea ice loss over this period. This is likely an upper bound on the contribution because previous studies found values between roughly one-third and one-half [(44% (Kay et al. 2011), 43%–53% (Stroeve et al. 2007), 33%–48% (Stroeve et al. 2012), and 30%–50% (Ding et al. 2017)]. Over the longer period 1958–2017 considered here, the contribution of internal variability is lower in the CESM-LE [24%; the ensemble mean trend is $-0.38 \times 10^6 \, \text{km}^2 \, (10 \, \text{yr})^{-1}$ as compared with the observed trend of $-0.50 \times 10^6 \, \text{km}^2 \, (10 \, \text{yr})^{-1}$]. This is consistent with the expectation that longer trends would show a smaller contribution from internal variability (Hawkins and Sutton 2011; Kay et al. 2011). In addition, the larger contribution of internal variability for 1979–2017 than 1958–2017 likely also reflects the increasing internal variability with decreasing mean ice extents [see Fig. S5 of both Swart et al. (2015) and Jahn (2018)]. We note that the same relationship does not necessarily hold for sea ice thickness or volume (Massonnet et al. 2018; Mioduszewski et al. 2019).

b. Regional sea ice trends and internal variability

To address the main question of this study regarding sea ice loss on a regional scale, we now move away from pan-Arctic metrics to examine spatial fields. The spatial structure of the sea ice concentration change over the historical period found in the CESM-LE simulations matches the pattern found in observations very well, and the observed change is within the range of 50-yr changes that, according to the CESM-LE, could possibly have occurred (Fig. 7). The CESM-LE ensemble mean change, understood to be an estimate of the forced response, shows significantly smaller levels of sea ice loss
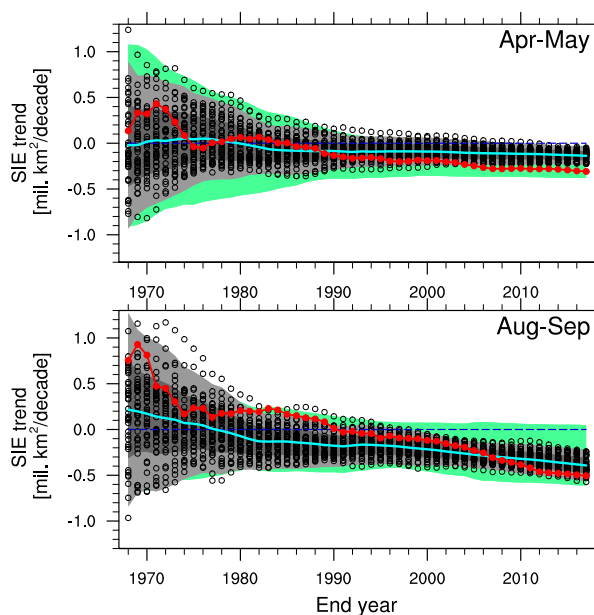

FIG. 5. Linear trends of Arctic sea ice extent that start from 1958 for the 40 members of the CESM-LE (black open circles), the CESM-LE ensemble mean (cyan line), and the observed value (red circles and line). The trends are of increasing lengths, with end years ranging from 1968 to 2017, reflecting trends of 10–50 yr. The dark-gray shading indicates values within 1 standard deviation of the ensemble mean, and the light-gray shading indicates within 2 standard deviations of the CESM ensemble mean. The green shading shows the 2σ envelope of trends found in the CMIP5 model ensemble. The blue dashed line shows the zero line. We divide the data into 2-month averages, with our focus in the study being April–May and August–September. Trends for every pair of months in a year are shown in online supplemental Fig. S1.

in all regions of the Arctic than the observations, in agreement with previous pan-Arctic studies (Kay et al. 2011; Stroeve et al. 2012). The observed 50-yr change in August–September sea ice fraction lies somewhere between -2σ and -1σ from the ensemble mean, and the observed 50-yr change in April–May sea ice fraction lies just outside -2σ from the ensemble mean. The wide range of changes simulated by CESM-LE highlights the large role of internal variability for regional sea ice cover changes, even for changes over half a century. If the effects of internal variability are distributed normally, which seems a relatively good assumption (Dai and Bloecker 2019), one would expect the change to fall within 2 standard deviations of the ensemble mean change roughly 95% of the time. For observed changes that lie outside the 2σ envelope, as is the case in April–May, this could indicate 1) that the forced response is not strong enough in the model, 2) that it is a very unlikely event we are seeing, and roughly 5% of changes should fall outside the envelope, 3) that the model could be getting the variability wrong, 4) observational
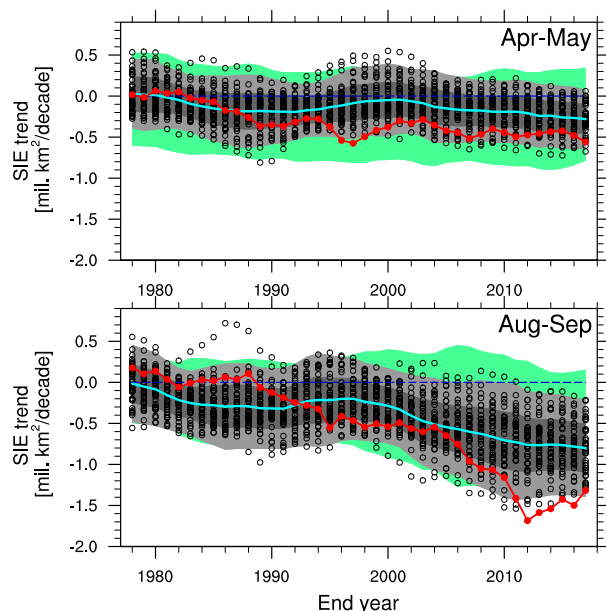
FIG. 6. Similar to Fig. 5, but for the 20-yr linear trends. The end year for these 20-yr trends ranges from 1978 to 2017. Trends for every pair of months in a year are shown in online supplemental Fig. S2.

uncertainties (Niederdrenk and Notz 2018), or 5) some combination of the preceding four.

Here it seems likely that option 1 is a likely candidate because the long-term trend for April–May is outside the range simulated by CESM-LE (Fig. 5). Although we have demonstrated that the CESM-LE outperforms CMIP5 models when examining the interannual variability of sea ice concentration (section 2d), the same is not necessarily true for the forced response (for which the "true" magnitude is challenging to assess). To assess the impact of the estimate of the forced response on the results shown in Fig. 7, we repeat the analysis replacing the CESM-LE ensemble mean with the CMIP5 multimodel mean, which provides another estimate of the forced response (Knutti 2010). We find, in agreement with Ding et al. (2019), that the CESM-LE ensemble mean has a faster rate of Arctic sea ice loss in the historical period than the CMIP5 ensemble mean and that the observed sea ice loss in April–May and August– September is outside the 2σ envelope if the CMIP5 mean is used (supplemental Fig. S3). We note that Rosenblum and Eisenman (2017) found that the CESM-LE ensemble mean has a lower rate of sea ice loss than the CMIP5 multimodel ensemble mean over a similar period. The difference is likely to arise from their study using every member from each CMIP5 model, giving a few models a much heavier weight. In this study we only use one member from each CMIP5 model, which follows

the "one model, one vote" approach used in the IPCC's model democracy (Knutti 2010).

The key finding of this paper is that for August–September the role of internal variability (section 2e) is nonuniform across the Arctic, both when the CESM-LE mean change is used to estimate the forced response (Fig. 8f) and when the CMIP5 multimodel mean change is used (Fig. 9f). In the CESM-LE, internal variability accounts for roughly 20%–50% of the observed sea ice loss across much of the Arctic, but in some hotspots it plays a greater role than anthropogenic forcing. These hotspots include the Laptev Sea, the East Beaufort Sea, and the Kara Sea and are mostly located leeward of islands such as Wrangel Island, the New Siberian Islands, and Svernaya Zemlya. The variability in the East Beaufort Sea and Laptev Sea is likely related to wind blowing the ice toward open waters causing a "loitering" of the sea ice edge (Steele and Ermold 2015). On the other hand, other regions, including the East Siberian Sea, the forced response accounts for nearly all of the observed change and internal variability plays a minimal role. Noting that the CMIP5 forced response in August–September is weaker than the CESM-LE response (cf. Figs. 8d and 9d), we deduce that the overall role for internal variability in driving the observed changes might be larger than the CESM-LE suggests. The contribution of internal variability (section 2e) when using the CMIP5 forced response is again found to be high in the Laptev Sea and Kara Sea. Generally, internal variability is shown to play an important role along the continental coastlines, whereas the forced response dominates closer to the pole. This is consistent with the fact that the climate change signal to noise ratio in August–September is order of magnitudes larger than in April–May, especially in the Arctic Ocean (Fig. S4 in the online supplemental material). We have repeated the analysis with a shorter time period (1979–88 to 2004–13) and a different observational dataset (Walsh et al. 2016) and the results were very similar (not shown).

In contrast with the results for the late summer, we find that in April–May internal variability is responsible for the vast majority (>75%) of recent observed sea ice changes (Figs. 8e, 9e). This result is not dependent on whether the forced response is estimated using the CESM-LE or the CMIP5 multimodel ensemble. Previous studies have highlighted the high levels of internal variability in the Barents Sea region (Smedsrud et al. 2013; Onarheim et al. 2015; Onarheim and Arthun 2017). Given that sea ice concentrations in the spring are highly correlated with sea ice conditions in the late winter in this region, our findings are consistent with previous studies that show the strong contribution of internal variability on decadal time scales, driven by
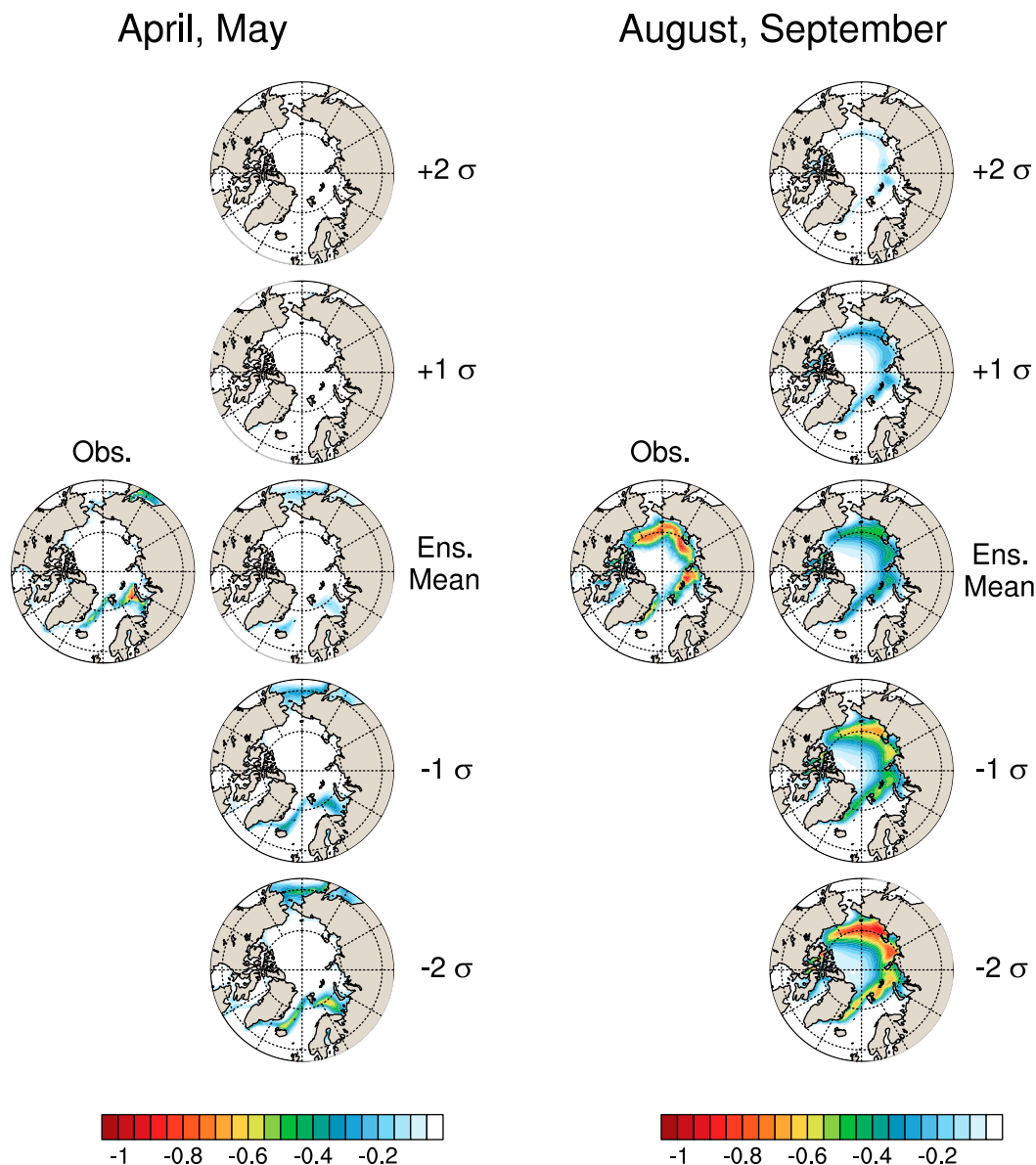
April, May

August, September

FIG. 7. Fifty-year changes in decadal means of Arctic sea ice fraction averaged over (left) April–May and (right) August–September from the HadISST datset ("Obs.") and ensemble mean ("Ens. Mean") of the 40-member CESM-LE. The decades of interest are 1958–67 and 2008–17. Multiples of the standard deviation (-2σ, -1σ, $+1\sigma$, and $+2\sigma$) are calculated from the 40 members and then added to the ensemble mean to demonstrate the 95% range of expected changes.

ocean heat transport, to winter sea ice loss (Smedsrud et al. 2013; Yeager et al. 2015). Because of the important role of internal variability, the signal-to-noise ratio of the climate change signal is orders of magnitude lower in April–May than in August–September in CESM-LE (supplemental Fig. S4). Therefore, the anthropogenically forced sea ice loss signal should be much easier to detect in August–September than in the late spring.

Last, we find that the spatial pattern of internal variability that we have just described is well explained by

the leading spatial modes of variability simulated by the CESM-LE. Figure 10 shows the two leading EOFs of 50-yr changes in the two seasons of interest, both for the control simulation and the historical period. Using the latitudinally weighted 50-yr change in decadal mean Arctic sea ice fraction, we calculate the EOFs across the 40 members of the CESM-LE (historical period) as well as overlapping 50-yr changes sampled across the 1800-yr control simulation (control period). These EOFs are the largest modes of variability to explain the spread in sea
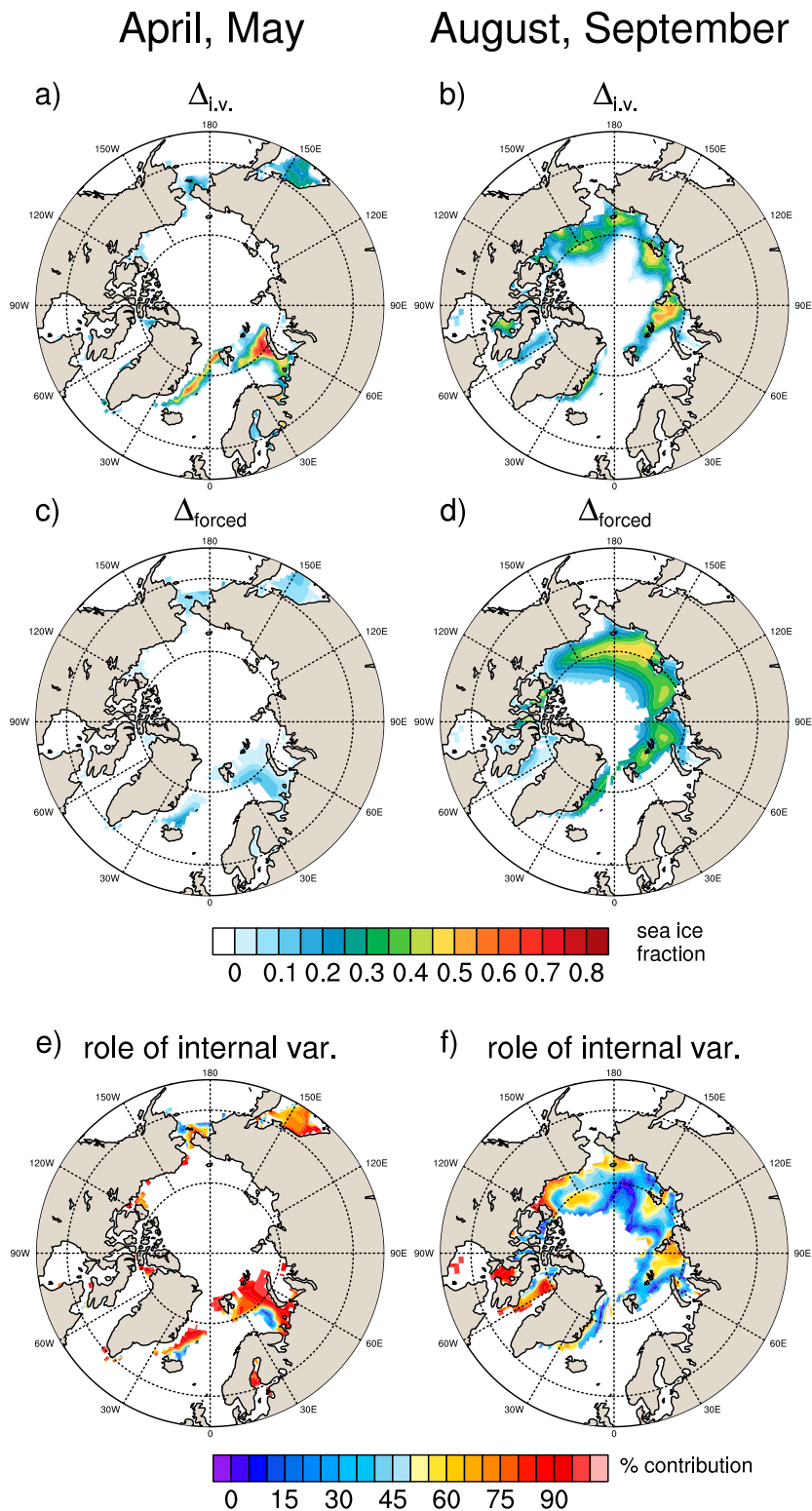
FIG. 8. For the 40 members of the CESM-LE, the contribution of (a),(b) internal variability and (c),(d) the forced response in (left) April–May and (right) August–September to the observed sea ice loss from 1958–67 to 2008–17 [shown in Fig. 7 ("Obs."), which is the sum of the top row and the middle row of this figure]. (e),(f) The percentage contribution of internal variability to the observed sea ice loss in each grid box, calculated as $100 \times [|\Delta_{iv}|/(\Delta_{iv} + \Delta_{forced})]$. An example of the calculation for one grid box is given in Fig. 4.
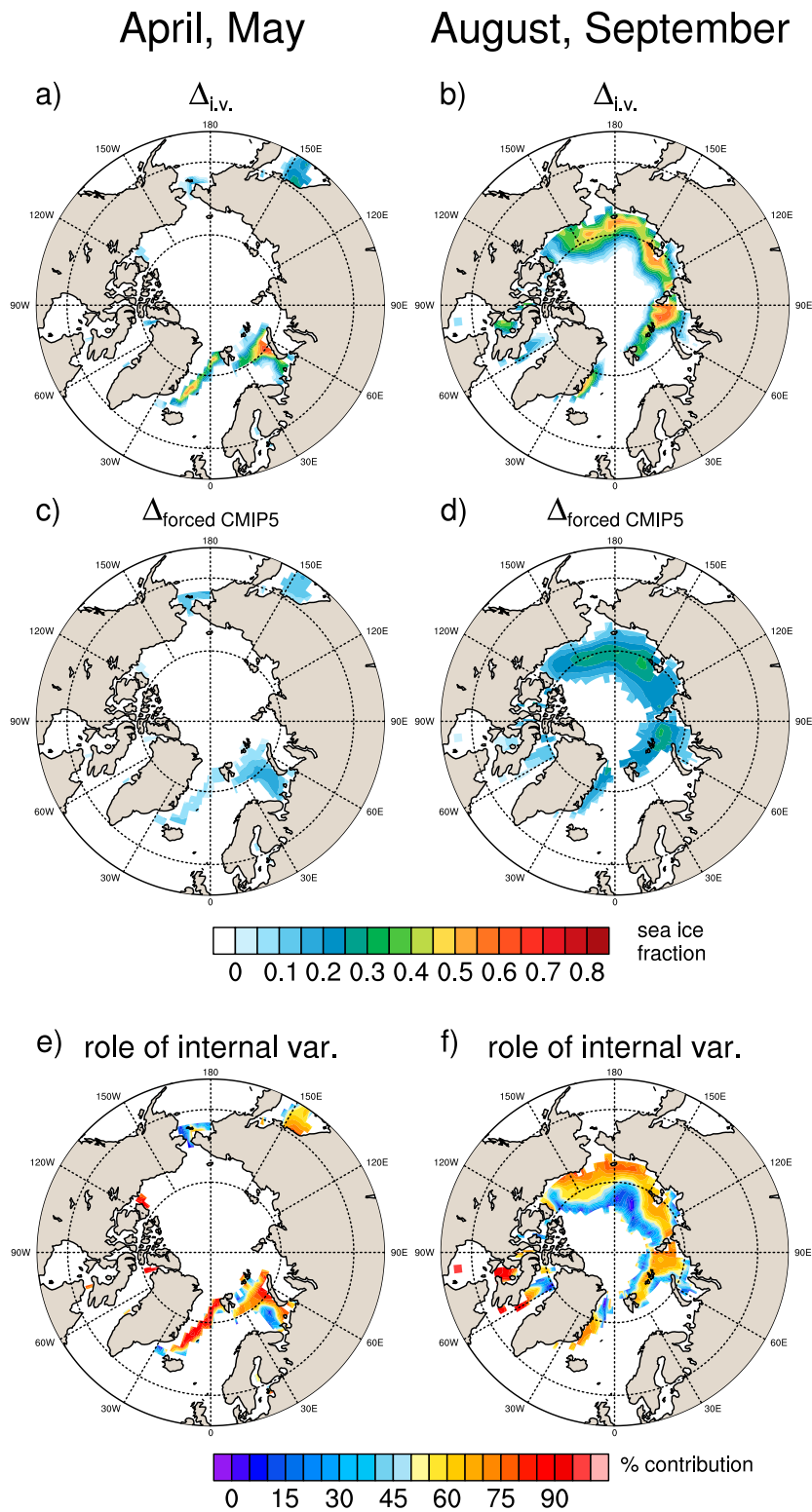
April, May

August, September

a) $\Delta_{\text{i.v.}}$

b) $\Delta_{\text{i.v.}}$

c) $\Delta_{\text{forced CMIP5}}$

d) $\Delta_{\text{forced CMIP5}}$

sea ice fraction

0   0.1 0.2 0.3 0.4 0.5 0.6 0.7 0.8

e) role of internal var.

f) role of internal var.

% contribution

0   15   30   45   60   75   90

FIG. 9. As in Fig. 8, but based upon the CMIP5 ensemble mean change (averaged from 32 CMIP5 models).
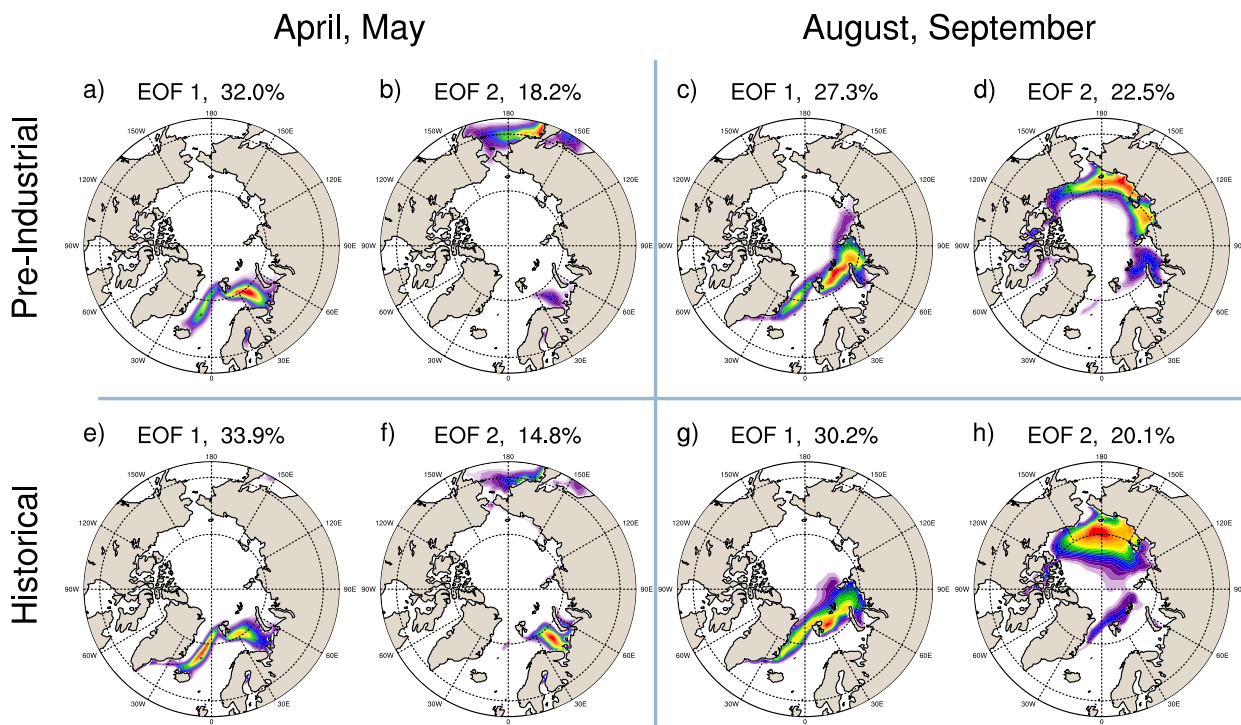
April, May   August, September

FIG. 10. The first two leading EOFs (normalized) of 50-yr changes in decadal means of Arctic sea ice fraction from (top) the CESM preindustrial control run and (bottom) from 1958–67 to 2008–17 from the CESM-LE. The control run provides 1741 overlapping 50-yr changes, and there are 40 independent 50-yr changes from the CESM-LE. We analyze the months (a),(b),(e),(f) April–May and (c),(d),(g),(h) August–September. The percentage of the total variance explained by the EOF is displayed, with the first two EOFs comprising one-half of the total variance. The remaining EOFs that are shown each account for less than 8% of the variance.

ice changes across the CESM-LE members. The first two EOFs in all seasons explain roughly one-half of the variance, and are well separated from each other. In April–May, the first and second EOFs are regionally focused on the Barents Sea; these describe the pattern of internal variability that is responsible for much of the observed sea ice loss in this region, although the first EOF is likely more important because of the lack of sea ice loss observed in the Bering Sea. In August–September the first two EOFs contribute roughly equally to the observed patterns of sea ice loss. Note that the difference in the second EOF in August–September between the preindustrial control to the historical period is the only EOF notably affected by the historical forcings. This is caused by the fact that in the historical period there is more sea ice variability farther poleward than in the preindustrial era, resulting from thicker and more extensive preindustrial sea ice cover.

4. Summary and discussion

Using the CESM-LE, we have demonstrated that internal variability has had a significant but spatially complex impact on recent historical Arctic sea ice loss. In fact,

our results indicate that the forced signal and large levels of internal variability could have combined to produce a wide range of trends, including a much reduced loss of Arctic sea ice concentration over the last half century ($+2\sigma$ event rather than a -2σ event). Focusing on the spatial pattern of internal variability, we demonstrated that the contribution of internal variability to changes in sea ice in late summer is highly nonuniform, accounting for less than 10% of the sea ice loss in the East Siberian Sea but more than 60% in the Kara Sea. Results for the spring are more uniform for the regions that have lost sea ice concentration, with a consistently large contribution of internal variability (>75%). This suggests that the observed recent sea ice loss in the Barents Sea is unlikely to have been caused by anthropogenic forcing; in fact, this region experiences the largest levels of internal variability, complicating and delaying the detection of a forced signal. Although it is in a different season, this raises the question of how much the proposed connection between winter Barents–Kara Sea sea ice loss and the midlatitudes (Kim et al. 2014; Zhang et al. 2018) is a forced response or driven by internal variability.

We have also shown that the nonuniform spatial patterns of internal variability are largely consistent

over time, based on EOF analysis of the CESM-LE historical period and the preindustral control run. The one exception to this is the second mode of variability in the late summer, when the changing sea ice state allows sea ice variability to encroach farther poleward into regions previously covered by year-round sea ice. The fact that the mode, which explains the most variance among sea ice trends, remains unchanged between the preindustrial and historical period, showing no imprint of climate change, highlights the important role of internal variability for the spatial pattern of Arctic sea ice change.

When considering the robustness of our results, it is important to keep in mind that the CESM-LE is only one model and our conclusions are only as reliable as the internal variability and forced response generated by the model. Among the currently available CMIP5-class models, the CESM-LE performs best for the metrics used in this study: the spatial structure and magnitude of recent changes and interannual variability. In particular, we showed that the spatial structure of interannual variability simulated by the CESM-LE is closer to observations than other CMIP5 models. We also showed that the observed trend in spring and summer sea ice extent mostly lies within the range of trends simulated by the CESM-LE for both shorter (20 yr) and longer (>30 yr) trends, with better performance in summer than spring. Furthermore, we showed that the results are similar whether we use the CESM-LE or CMIP5 forced trends. Therefore, as long as the change in ensemble mean is a good estimate of the forced response to recent climate change, the results are robust. However, it has been suggested that the annual-mean sea ice sensitivity in the CESM-LE and CMIP5 models, and hence the simulation of the forced response, might be too low (Notz and Stroeve 2016; Rosenblum and Eisenman 2017). If that is the case, the role on internal variability might be overestimated. However, Ding et al. (2019) offer evidence that models do not underestimate sea ice sensitivity, but instead are not able to represent realistic polar–tropical linkages, which affect the global temperatures. Furthermore, observational estimates of the sensitivity of Arctic sea ice to emissions and global temperature are associated with large uncertainties (Niederdrenk and Notz 2018). For September, it has been shown that the CESM-LE sea ice sensitivity is consistent with some observational data, but too weak when other data is used (Jahn 2018). Hence, as far as we can assess the models at present, our results are the best estimate of the contribution of internal variability to Arctic sea ice loss. Nonetheless, the CESM-LE still shows some biases that might affect the results and that limit the months of the year that we can study with it. For

example, it has been suggested that the CESM-LE underestimates variability in the North Atlantic (Kim et al. 2018), which is likely connected to the Atlantic inflow and sea ice concentration in the Barents Sea (Li et al. 2017). Even small biases in the atmospheric circulation can contribute to uncertainty in this region (Park et al. 2015; DeRepentigny et al. 2016).

To conclude, our analysis provides the first spatial assessment of the role of internal variability on the observed sea ice loss. It shows that the imprint of internal variability is highly nonuniform, both in time and in space. While several previous studies (Kay et al. 2011; Stroeve et al. 2007, 2012; Zhang 2015; Ding et al. 2017, 2019) have shown a large contribution of internal variability to the observed pan-Arctic sea ice loss, our study demonstrates that regionally the contribution of internal variability can be as little as 10% and as much as 75%, depending on the month and region in question. In this study we have examined sea ice concentration, but results may be different for sea ice thickness and multiyear sea ice (Kwok 2018; Massonnet et al. 2018; Mioduszewski et al. 2019). These results are important for stakeholders to interpret spatial sea ice predictions and projections, as regions and times of the year that show high internal variability in the sea ice cover are less predictable than regions with small internal variability.

paper are archived on the High Performance Storage System at the National Center for Atmospheric Research, and can be provided upon request. We acknowledge Environment and Climate Change Canada's Canadian Centre for Climate Modelling and Analysis for executing and making available the CanESM2 Large Ensemble simulations used in this study and the Canadian Sea Ice and Snow Evolution Network for proposing the CanESM2 Large Ensemble.

REFERENCES

Barnes, E., and R. Barnes, 2015: Estimating linear trends: Simple linear regression versus epoch differences. *J. Climate*, **28**, 9969–9976, https://doi.org/10.1175/JCLI-D-15-0032.1.

Barnhart, K., C. Miller, I. Overeem, and J. Kay, 2016: Mapping the future expansion of Arctic open water. *Nat. Climate Change*, **6**, 280–285, https://doi.org/10.1038/nclimate2848.

Comiso, J., C. Meier, and R. Gersten, 2017: Variability and trends in the Arctic sea ice cover: Results from different techniques. *J. Geophys. Res. Oceans*, **122**, 6883–6900, https://doi.org/10.1002/2017JC012768.

Dai, A., and C. Bloecker, 2019: Impacts of internal variability on temperature and precipitation trends in large ensemble simulations by two climate models. *Climate Dyn.*, **52**, 289–306, https://doi.org/10.1007/s00382-018-4132-4.

DeRepentigny, P., B. Tremblay, R. Newton, and S. Pfirman, 2016: Patterns of sea ice retreat in the transition to a seasonally ice-free Arctic. *J. Climate*, **29**, 6993–7008, https://doi.org/10.1175/JCLI-D-15-0733.1.

Ding, Q., and Coauthors, 2017: Influence of high-latitude atmospheric circulation changes on summertime Arctic sea ice. *Nat. Climate Change*, **7**, 289–295, https://doi.org/10.1038/nclimate3241.

——, and Coauthors, 2019: Fingerprints of internal drivers of Arctic sea ice loss in observations and model simulations. *Nat. Geosci.*, **12**, 28–33, https://doi.org/10.1038/s41561-018-0256-8.

Frankcombe, L., M. England, J. Kajtar, M. Mann, and B. Steinman, 2018: On the choice of ensemble mean for ensemble mean for estimating the forced signal in the presence of internal variability. *J. Climate*, **31**, 5681–5693, https://doi.org/10.1175/JCLI-D-17-0662.1.

Hawkins, E., and R. Sutton, 2011: Time of emergence of climate signals. *Geophys. Res. Lett.*, **39**, L01702, https://doi.org/10.1029/2011GL050087.

Hurrell, J., and Coauthors, 2013: The Community Earth System Model: A framework for collaborative research. *Bull. Amer. Meteor. Soc.*, **94**, 1339–1360, https://doi.org/10.1175/BAMS-D-12-00121.1.

Jahn, A., 2018: Reduced probability of ice-free summers for 1.5°C compared to 2°C warming. *Nat. Climate Change*, **8**, 409–413, https://doi.org/10.1038/s41558-018-0127-8.

——, J. Kay, M. Holland, and D. Hall, 2016: How predictable is the timing of a summer ice-free Arctic? *Geophys. Res. Lett.*, **43**, 9113–9120, https://doi.org/10.1002/2016GL070067.

Kay, J., M. Holland, and A. Jahn, 2011: Inter-annual to multidecadal Arctic sea ice extent trends in a warming world. *Geophys. Res. Lett.*, **38**, L15708, https://doi.org/10.1029/2011GL048008.

——, and Coauthors, 2015: The Community Earth System Model (CESM) Large Ensemble project: A community resource for studying climate change in the presence of internal climate variability. *Bull. Amer. Meteor. Soc.*, **96**, 1333–1349, https://doi.org/10.1175/BAMS-D-13-00255.1.

Kim, B., S. Son, S. Min, J. Jeong, S. Kim, X. Zhang, T. Shim, and J. Yoon, 2014: Weakening of the stratospheric polar vortex by Arctic sea-ice loss. *Nat. Commun.*, **5**, 4646, https://doi.org/10.1038/ncomms5646.

Kim, W., S. Yeager, P. Chang, and G. Danabasoglu, 2018: Low-frequency North Atlantic climate variability in the Community Earth System Model Large Ensemble. *J. Climate*, **31**, 787–813, https://doi.org/10.1175/JCLI-D-17-0193.1.

Knutti, R., 2010: The end of model democracy? *Climatic Change*, **102**, 395–404, https://doi.org/10.1007/s10584-010-9800-2.

Kwok, R., 2018: Arctic sea ice thickness, volume, and multiyear ice coverage: Losses and coupled variability (1958–2018). *Environ. Res. Lett.*, **13**, 105005, https://doi.org/10.1088/1748-9326/aae3ec.

——, and D. Rothrock, 2009: Decline in Arctic sea ice thickness from submarine and ICESat records: 1958–2008. *Geophys. Res. Lett.*, **36**, L11501, https://doi.org/10.1029/2009GL039035.

Labe, Z., G. Magnusdottir, and H. Stern, 2018: Variability of Arctic sea ice thickness using PIOMAS and the CESM large ensemble. *J. Climate*, **31**, 3233–3247, https://doi.org/10.1175/JCLI-D-17-0436.1.

Lahn, G., and C. Emmerson, 2012: Arctic opening: Opportunity and risk in the high north. Tech. Rep., Chatham House, 60 pp., https://www.chathamhouse.org/publications/papers/view/182839.

Lamarque, J., and Coauthors, 2010: Historical (1850–2000) gridded anthropogenic and biomass burning emissions of reactive gases and aerosols: Methodology and application. *Atmos. Chem. Phys.*, **10**, 7017–7039, https://doi.org/10.5194/acp-10-7017-2010.

Li, D., R. Zhang, and T. Knutson, 2017: On the discrepancy between observed and CMIP5 multi-model simulated Barents Sea winter sea ice decline. *Nat. Commun.*, **8**, 14991, https://doi.org/10.1038/ncomms14991.

Lindsay, R., and A. Schweiger, 2015: Arctic sea ice thickness loss determined using subsurface, aircraft, and satellite observations. *Cryosphere*, **9**, 269–283, https://doi.org/10.5194/tc-9-269-2015.

Liu, J., M. Song, R. Horton, and Y. Hu, 2013: Reducing spread in climate model projections of a September ice-free Arctic. *Proc. Natl. Acad. Sci. USA*, **110**, 12 571–12 576, https://doi.org/10.1073/pnas.1219716110.

Massonnet, F., M. Vancoppenolle, H. Goosse, D. Docquier, T. Fichefet, and E. Blanchard-Wrigglesworth, 2018: Arctic sea-ice change tied to its mean state through thermodynamic processes. *Nat. Climate Change*, **8**, 599–603, https://doi.org/10.1038/s41558-018-0204-z.

McKinnon, K., and C. Deser, 2018: Internal variability and regional climate trends in an observational large ensemble. *J. Climate*, **31**, 6783–6802, https://doi.org/10.1175/JCLI-D-17-0901.1.

——, A. Poppick, E. Dunn-Sigouin, and C. Deser, 2017: An "observational large ensemble" to compare observed and modeled temperature trend uncertainty due to internal variability. *J. Climate*, **30**, 7585–7598, https://doi.org/10.1175/JCLI-D-16-0905.1.

Meinshausen, M., and Coauthors, 2011: The RCP greenhouse gas concentrations and their extensions from 1765 to 2300. *Climatic Change*, **109**, 213–241, https://doi.org/10.1007/s10584-011-0156-z.

Mioduszewski, J., S. Vavrus, M. Wang, M. Holland, and L. Landrum, 2019: Past and future interannual variability in

Arctic sea ice in coupled climate model. *Cryosphere*, **13**, 113–124, https://doi.org/10.5194/tc-13-113-2019.

Niederdrenk, A., and D. Notz, 2018: Arctic sea ice in a 1.5°C warmer world. *Geophys. Res. Lett.*, **45**, 1963–1971, https://doi.org/10.1002/2017GL076159.

Notz, D., and J. Stroeve, 2016: Observed Arctic sea ice loss directly follows anthropogenic CO_2 emission. *Science*, **354**, 747–750, https://doi.org/10.1126/science.aag2345.

Onarheim, I., and M. Arthun, 2017: Toward an ice-free Barents Sea. *Geophys. Res. Lett.*, **44**, 8387–8395, https://doi.org/10.1002/2017GL074304.

——, T. Eldevik, M. Arthun, R. Ingvaldsen, and L. Smedsrud, 2015: Skillful prediction of Barents Sea ice cover. *Geophys. Res. Lett.*, **42**, 5364–5371, https://doi.org/10.1002/2015GL064359.

——, ——, L. Smedsrud, and J. Stroeve, 2018: Seasonal and regional manifestation of Arctic sea ice loss. *J. Climate*, **31**, 4917–4932, https://doi.org/10.1175/JCLI-D-17-0427.1.

Overland, J., and M. Wang, 2013: When will the summer Arctic be nearly sea ice free? *Geophys. Res. Lett.*, **40**, 2097–2101, https://doi.org/10.1002/grl.50316.

Park, D., S. Lee, and S. Feldstein, 2015: Attribution of the recent winter sea ice decline over the Atlantic sector. *J. Climate*, **28**, 4027–4033, https://doi.org/10.1175/JCLI-D-15-0042.1.

Rosenblum, E., and I. Eisenman, 2017: Sea ice trends in climate models only accurate in runs with biased global warming. *J. Climate*, **30**, 6265–6278, https://doi.org/10.1175/JCLI-D-16-0455.1.

Sigmond, M., J. Fyfe, and N. Swart, 2018: Ice-free Arctic projections under the Paris Agreement. *Nat. Climate Change*, **8**, 404–408, https://doi.org/10.1038/s41558-018-0124-y.

Smedsrud, L., and Coauthors, 2013: The role of the Barents Sea in the Arctic climate system. *Rev. Geophys.*, **51**, 415–449, https://doi.org/10.1002/rog.20017.

Steele, M., and W. Ermold, 2015: Loitering of the retreating sea ice edge in the Arctic Seas. *J. Geophys. Res.*, **120**, 7699–7721, https://doi.org/10.1002/2015JC011182.

Stroeve, J., and D. Notz, 2018: Changing state of Arctic sea ice across all seasons. *Environ. Res. Lett.*, **13**, 103001, https://doi.org/10.1088/1748-9326/aade56.

——, M. Holland, W. Meier, T. Scambos, and M. Serreze, 2007: Arctic sea ice decline: Faster than forecast. *Geophys. Res. Lett.*, **34**, L09501, https://doi.org/10.1029/2007GL029703.

——, V. Kattsov, A. Barrett, M. Serreze, T. Pavlova, M. Holland, and W. Meier, 2012: Trends in Arctic sea ice extent from CMIP5, CMIP3 and observations. *Geophys. Res. Lett.*, **39**, L16502, https://doi.org/10.1029/2012GL05267.

——, A. Barrett, M. Serreze, and A. Schweiger, 2014a: Changes in Arctic melt season and implications for sea ice loss. *Geophys. Res. Lett.*, **41**, 1216–1225, https://doi.org/10.1002/2013GL058951.

——, ——, ——, and ——, 2014b: Using records from submarine, aircraft and satellite to evaluate climate model simulations of Arctic sea ice thickness. *Cryosphere*, **8**, 1839–1854, https://doi.org/10.5194/tc-8-1839-2014.

Swart, N., J. Fyfe, E. Hawkins, J. Kay, and A. Jahn, 2015: Influence of internal variability on Arctic sea-ice trends. *Nat. Climate Change*, **5**, 86–89, https://doi.org/10.1038/nclimate2483.

Taylor, K., R. Stouffer, and G. Meehl, 2012: An overview of CMIP5 and the experiment design. *Bull. Amer. Meteor. Soc.*, **93**, 485–498, https://doi.org/10.1175/BAMS-D-11-00094.1.

Thompson, D., E. Barnes, C. Deser, W. Foust, and A. Phillips, 2015: Quantifying the role of internal climate variability in future climate trends. *J. Climate*, **28**, 6443–6456, https://doi.org/10.1175/JCLI-D-14-00830.1.

Titchner, H., and N. Rayner, 2014: The Met Office Hadley Centre sea ice and sea surface temperature data set, version 2.1: Sea ice concentrations. *J. Geophys. Res. Atmos.*, **119**, 2864–2889, https://doi.org/10.1002/2013JD020316.

Walsh, J., W. Chapman, and F. Fetterer, 2016: Gridded monthly sea ice extent and concentration, 1850 onward, version 1. NSIDC, accessed 15 February 2019, https://doi.org/10.7265/N5833PZ5.

Yeager, S., A. Karspeck, and G. Danabasoglu, 2015: Predicted slowdown in the rate of Atlantic sea ice loss. *Geophys. Res. Lett.*, **42**, 10 704–10 713, https://doi.org/10.1002/2015GL065364.

Zhang, P., Y. Wu, I. Simpson, K. Smith, X. Zhang, B. De, and P. Callaghan, 2018: A stratospheric pathway linking a colder Siberia to Barents–Kara Sea sea ice loss. *Sci. Adv.*, **4**, eaat6025, https://doi.org/10.1126/sciadv.aat6025.

Zhang, R., 2015: Mechanisms for low-frequency variability of summer Arctic sea ice extent. *Proc. Natl. Acad. Sci. USA*, **112**, 4570–4575, https://doi.org/10.1073/pnas.1422296112.